Chin. Geogra. Sci. 2019 Vol. 29 No. 6 pp. 905–916
https://doi.org/10.1007/s11769-019-1080-9

Springer Science Press
www.springerlink.com/content/1002-0063

Monitoring Intra-annual Spatiotemporal Changes in Urban Heat Islands in 1449 Cities in China Based on Remote Sensing

LI Yuanzheng[1, 2, 3], WANG Lan[4], ZHANG Liping[5], LIU Min[1, 3], ZHAO Guosong[6]

(1. *School of Resources and Environment*, *Henan University of Economics and Law*, *Zhengzhou* 450046, *China*; 2. *Academician Laboratory for Urban and Rural Spatial Data Mining of Henan Province*, *Henan University of Economics and Law*, *Zhengzhou* 450046, *China*; 3. *State Key Laboratory of Urban and Regional Ecology*, *Research Center for Eco-Environmental Sciences*, *Chinese Academy of Sciences*, *Beijing* 100085, *China*; 4. *Key Laboratory of Urban Environment and Health*, *Institute of Urban Environment*, *Chinese Academy of Sciences*, *Xiamen* 361021, *China*; 5. *Center for Environmental Zoning*, *Chinese Academy for Environmental Planning*, *Ministry of Environmental Protection of China*, *Beijing* 100012, *China*; 6. *Key Laboratory of Land Surface Pattern and Simulation*, *Institute of Geographic Sciences and Natural Resources Research*, *Chinese Academy of Sciences*, *Beijing* 100101)

Abstract: This study aimed to accurately study the intra-annual spatiotemporal variation in the surface urban heat island intensities (SUHIIs) in 1449 cities in China. First, China was divided into five environmental regions. Then, the SUHIIs were accurately calculated based on the modified definitions of the city extents and their corresponding nearby rural areas. Finally, we explored the spatiotemporal variation of the mean, maximum, and minimum values, and ranges of SUHIIs from several aspects. The results showed that larger annual mean daytime SUHIIs occurred in hot-humid South China and cold-humid northeastern China, and the smallest occurred in arid and semiarid west China. The seasonal order of the SUHIIs was summer > spring > autumn > winter in all the temperate regions except west China. The SUHIIs were obviously larger during the rainy season than the dry season in the tropical region. Nevertheless, significant differences were not observed between the two seasons within the rainy or dry periods. During the daytime, the maximum SUHIIs mostly occurred in summer in each region, while the minimum occurred in winter. A few cold island phenomena existed during the nighttime. The maximum SUHIIs were generally significantly positively correlated with the minimum SUHIIs during the daytime, nighttime and all-day in all environmental regions throughout the year and the four seasons. Moreover, significant correlation scarcely existed between the daytime and nighttime ranges of the SUHIIs. In addition, the daytime SUHIIs were also insignificantly correlated with the nighttime SUHIIs in half of the cases.

Keywords: surface urban heat island intensities (SUHIIs); land surface temperature (LST); seasonal changes; maximum and minimum SUHII; cold island; China

Citation: LI Yuanzheng, WANG Lan, ZHANG Liping, LIU Min, ZHAO Guosong, 2019. Monitoring Intra-annual Spatiotemporal Changes in Urban Heat Islands in 1449 Cities in China Based on Remote Sensing. *Chinese Geographical Science*, 29(6): 905–916. https://doi.org/10.1007/s11769-019-1080-9

1 Introduction

In 2018, 55% of the world's population lived in urban areas and this proportion is expected to reach 68% in 2050 (UN DESA PD, 2018). Rapid, high-intensity urbanization has obviously changed the ecology and environment at urban, regional, and even global scales. One of the most obvious urban climate features is the urban heat island effect (UHI) (Howard, 1833), which can directly and indirectly affect regional climate (Filho

Received date: 2019-03-08; accepted date: 2019-06-24

Foundation item: Under the auspices of National Natural Science Foundation of China (No. 41901238, 41701501), Social Science Fund of China (General Projects) (No.17BJL065), Key Scientific and Technological Project of Henan Province (No. 192102310003), Educational Commission of Henan Province (No. 2019-ZZJH-094)

Corresponding author: LIU Min. E-mail: liuminrcees@126.com

et al., 2017), energy use (Zinzi et al., 2018), air quality (Chen et al., 2018), urban hydrology (Richards and Edwards, 2018), soil physicochemical properties (Shi et al., 2012), creature distribution and activities (Sfîcă et al., 2017), and human health, comfort and quality of life (Lee et al., 2017).

Although land surface temperatures (LSTs) derived by remote sensing are not identical to above-ground air temperatures, they are closely related (Mostovoy et al., 2006; Schwarz et al., 2011). Nonetheless, UHIs are called 'surface urban heat islands' when derived from remote sensing data in order to distinguish them from traditional UHIs analyzed using air temperatures (Voogt and Oke, 2003). The spatiotemporal changes in surface urban heat island intensities (SUHIIs) have been examined in many previous studies. The thermal infrared data sources adopted to investigate these changes include satellite-based and airborne-based types and thermal video radiometry (Li et al., 2016; Zhou et al., 2019). More than 30 indicators have been developed, and the methods can be classified into land cover driven approaches, LST pattern driven approaches, and a combination of the two approaches (Schwarz et al., 2012; Li et al., 2019). Various spatiotemporal variation laws have been studied, including the intra-annual and interannual variations in the daytime and nighttime SUHIIs and comparisons between these variations at a single city, regional, continental, or global scale (Li et al., 2016).

Nevertheless, deficiencies still exist in the research (Li et al., 2016), and only some of these deficiencies are listed here. First, there are disadvantages related to the monitoring indices used in previous studies at the continental or global scales, such as the diverse and defective definitions of cities and villages and in some cases, the nonnormal distribution of LST (Li et al., 2019). Second, most of the previous studies have focused on the single city or regional city group scales, and usually used different indicators (Li et al., 2016). Nevertheless, weak correlations and poor comparability exist among the results derived by different indicators (Schwarz et al., 2011). The SUHIIs of various cities should be compared using the same indicator (Schwarz et al., 2012). Therefore, studies on the continental or global scale should be enhanced in order to understand the spatiotemporal variations laws accurately, clearly, and systematically. Third, the research has concentrated on large and mega cities, while few studies have focused on medium-sized and small cities (Li et al., 2016). Fourth, even fewer studies have focused on the spatiotemporal changes in maximum and minimum SUHII (Clinton and Gong, 2013). Finally, although the ecological context has an obvious impact on the spatiotemporal characteristics of SUHIIs, including water and heat combinations, vegetation characteristics, landforms, and human activities, etc. Nevertheless, most of previous studies did not consider this factor, or simply used administrative boundary data to determine regions with a different context.

Thus, the objective of this study is to use an improved monitoring index to study the intra-annual variability of the SUHIIs in 1449 cities in five regions with different ecological contexts in China. The specific objectives include the following: 1) to analyse the spatial-temporal rules of mean, maximum, and minimum values, and annual ranges of daytime and nighttime SUHIIs; 2) to do significance testing of SUHIIs between the daytime and nighttime, among the four seasons, and among the five environmental regions, respectively; and 3) to explore the correlations between the annual maximum and minimum SUHIIs during the daytime, nighttime and all-day, between the annual daytime and nighttime SUHIIs ranges, between the mean daytime and nighttime SUHIIs in each season and throughout the year in China and among the five regions of China, respectively.

2 Materials and Methods

2.1 Study area

China was divided into five regions based on the ecological function recognition results for the first, second and third levels (Fig. 1) to analyse the potential different spatiotemporal variations of SUHIIs in each region. Region I mainly corresponded to the vast majority of the northeastern China, which has climatic zones that range from cold temperate to mid-temperate. The region is affected by monsoons and has four distinct seasons, i.e., warm and rainy summers and cold and dry winters, and has long periods of melting ice and snow. The climate of region II is similar to that of region I. However, winters are warmer and shorter than those in region I. Region III is the only zone that is not affected by monsoons in China which has a typical arid temperate climate, a mean annual precipitation (MAP) below 400 mm, and cold winters and hot or warm summers. The vast majority

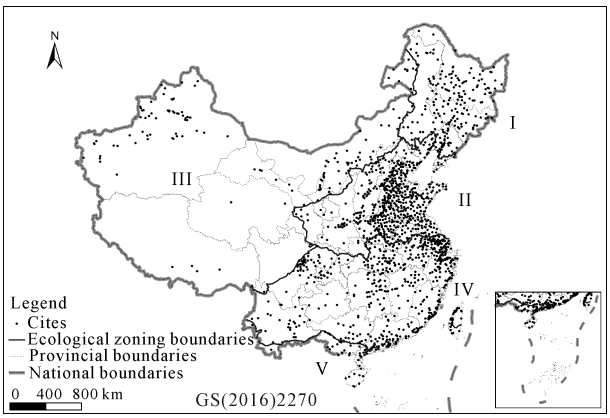

Fig. 1 Locations of the 1449 cities used for this study in five environmental subareas in China in 2010

of region IV belongs to the subtropical zone, and the rest is in the tropical zone. This region has a typical rainy and hot temperate climate, with MAP exceeding 800 mm and evergreen vegetation.

2.2 Data

Monthly mean LST data at a 1-km resolution from MODIS/Aqua were downloaded from the Geospatial Cloud of Computer Network Information Centre, Chinese Academy of Sciences (http://www.gscloud.cn/). Each pixel value was a simple average of all the corresponding MYD11A1 LST pixels collected within that month period. The MYD11A1 product uses the split-window technique to derive LSTs. Land use data from 2010 at a 1-km resolution, were provided by the Data Centre for Resources and Environmental Sciences, Chinese Academy of Sciences (http://www.resdc.cn), and they were primarily produced from the interpretation of Landsat TM/ETM+ images (Liu et al., 2014). Their classification schemes include six first-level land use types: cropland, woodland, grassland, waterbody, built-up land, and unused land (Liu et al., 2005; Zhang et al., 2014). In addition, 25 second-level land use types are included in these two data sets, and their overall accuracy of classification is more than 91.2% for each land use type (Liu et al., 2014; Zhang et al., 2014). The 500-m resolution impervious percentage data for 2010 were provided by the Beijing City Lab (https://www.beijingcitylab.com/), and they were derived by regression method, based on the normalized urban areas composite index (NUACI) (Liu et al., 2015). The NUACI was produced by nighttime light intensity, enhanced vegetation index and normalized difference water index (Liu et al., 2015). The accuracy of impervious surface percentage data is high (R^2 = 0.8079, *RMSE* = 0.1176), having referring to the extracted impervious data by the maximum likelihood method using the data obtained by Enhanced Thematic Mapper plus (ETM+) in Landsat satellites (Liu et al., 2015).

Ecological function recognition data were provided by the Data Sharing Infrastructure of Urban and Regional Ecological Science (http://dse.rcees.cas.cn/). China was divided into three first-level, 50 second-level, 206 third-level, and 1434 fourth-level ecological function regions based on their landforms, water and heat combinations, and vegetation characteristics.

2.3 Methods

2.3.1 Definition of urban and rural regions

The urban land polygons were first aggregated at a distance of 1 km, which is sufficient to include most adjacent and scattered urban land polygons into the urban class and is able to separate the main city zones and satellite cities or two closely adjacent cities that should be considered separately according to normal human perceptions. Cities with areas larger than 6 km^2 were considered, which included the vast majority of cities in the eastern regions in China and those with the densest populations and most well-developed economies. The corresponding rural zones were defined as the buffer zones of cities, with buffer distances between 5 and 10 km (Clinton and Gong, 2013) and impervious percentages below 5% (Imhoff et al., 2010; Zhang et al., 2010); however, the rural zones do not include waterbodies, regions with slopes exceeding 7.5°, or elevations that are 50 m greater than the maximum elevation or less than the minimum elevation of the urban zones, respectively (Imhoff et al., 2010; Zhou et al., 2015; Zhou et al., 2016). We found that 99.70% of the cities in China in 2010 were in plain regions with slopes under 7.5°.

2.3.2 Calculation of SUHIIs and analysis of its intra-annual spatio-temporal changes

The seasons were defined based on the definitions of meteorological seasons (Ren et al., 2005). Winter ranges from December to February, spring ranges from March to May, summer ranges from June to August, and autumn ranges from September to November. First, the mean daytime and nighttime SUHIIs, the seasonal and yearly differences in SUHIIs, the annual maximum and

minimum values, their occurring seasons, and the annual ranges of the SUHIIs during the daytime, nighttime, and all-day were calculated for each city. Then, the basic statistics for the above-mentioned indices were calculated. Significant differences in the SUHIIs were observed between the daytime and nighttime as well as among the four seasons and the five environmental regions, and these differences were determined using nonparametric tests of two samples, *K* dependent samples, and *K* independent samples. Third, to quantify whether the maximum and minimum values would occur in the same place, Spearman correlation coefficients were calculated between the annual maximum and minimum SUHIIs during the daytime, nighttime, or all-day in the five environment regions and throughout China. Moreover, the Spearman correlation coefficients were calculated between the annual ranges of the SUHIIs during the daytime and nighttime and between the mean daytime and nighttime SUHIIs in each season and throughout the year in China as a whole and its five environmental regions.

3 Results and Discussion

3.1 Spatiotemporal changes of SUHII

3.1.1 Spatiotemporal changes in daytime SUHII

From the annual aspect, 91.34% cities had positive SUHII values (Table 1). In China, the vast majority of cities had positive annual SUHII values while negative SUHII values were concentrated in region III and its surrounding regions (Fig. 2a), which had arid and semi-arid climates. This result was consistent with previous studies (Tran et al., 2006; Zhang et al., 2010; Peng et al., 2011; Lazzarini et al., 2013; Zhao et al., 2014; Haashemi et al., 2016). The minimum SUHII value existed in region III where the climate was arid and semi-arid (Figs. 2a and 3a). Higher SUHII values occurred in regions IV and V where the climate was hot-humid or in region I where the climate was cold-humid (Fig. 3a). This result supported previous studies (Zhao et al., 2014; Zhou et al., 2014), but there were still some differences. The highest daytime SUHII values did not occur in region I but in two southern

Table 1 The proportion of positive surface urban heat island intensities (SUHIIs) in China and in the five environmental regions throughout the year and during the four seasons in 2010 (%)

Indices	Period	China	Region I	Region II	Region III	Region IV	Region V
Annual mean	Day	91.34	91.00	93.74	60.90	96.19	97.67
	Night	96.54	93.50	99.08	96.99	94.69	100.00
	Day-night	55.47	59.00	38.67	25.56	77.52	74.42
Winter mean	Day	61.85	72.00	37.20	58.65	81.21	97.73
	Night	90.05	90.50	96.13	93.98	82.35	93.18
	Day-night	35.18	32.50	13.63	29.32	58.25	54.55
Spring mean	Day	85.56	79.50	87.11	57.89	93.36	84.09
	Night	94.61	94.50	99.08	96.24	89.75	93.18
	Day-night	67.10	57.50	62.98	31.58	84.82	56.82
Summer mean	Day	91.00	94.00	97.97	54.14	92.19	88.37
	Night	95.99	92.00	98.90	97.74	94.31	93.18
	Day-night	79.71	88.00	87.48	38.35	79.43	74.42
Autumn mean	Day	86.45	77.00	88.40	44.36	97.53	100.00
	Night	93.57	82.50	97.97	92.48	92.98	100.00
	Day-night	50.79	55.50	27.44	16.54	78.56	88.64
Annual maximum	Day	97.65	99.00	99.08	84.21	98.86	100.00
	Night	98.96	95.50	100.00	99.25	99.05	100.00
	All-day	100.00	100.00	100.00	100.00	100.00	100.00
Annual minimum	Day	49.58	49.50	31.31	21.05	73.90	72.09
	Night	84.04	78.00	94.48	86.47	74.76	86.36
	All-day	40.10	42.00	28.91	17.29	54.86	62.79

Notes: The annual mean, winter mean, spring mean, summer mean and autumn mean indicate the mean SUHIIs throughout the year and in the corresponding seasons. The annual maximum and minimum refer to the maximum and minimum SUHIIs throughout the year. Day, night and all-day represent the SUHIIs during the daytime, nighttime and the whole day, respectively. Day-night means the differences between daytime and nighttime SUHIIs.

regions without significant differences between them. Similarly, there was an insignificant difference between the SUHII values in regions I and V. Due to the large number of cities in this study, the strongest SUHII values were found to mainly occur in the cities in the Yangtze River Delta and coastal areas of Taiwan (Fig. 2a).

There were obvious seasonal variations in the SUHII values in cities with temperate and subtropical climates (Figs. 2b–2e and 3a). In addition, the SUHII values were in the order of summer > spring > autumn > winter in all temperate regions except for the arid and semi-arid region III. In this region, only the SUHII in the autumn was significantly different from the other seasons when it exhibited the lowest negative mean value. Note the minimum SUHII occurred in the winter in six major cities in the southwestern China (Zhou et al., 2016), and in Abu Dhabi, which has a typical desert climate (Lazzarini et al., 2013). A total of 133 cities in southeastern China were examined in this study. The ecological borders were determined mainly based on landform, climate, vegetation characteristics, *etc*., rather than provincial borders, as was done in previous studies. The minimum SUHII did not occur in the winter in region III likely because of the influence of the accumulation of hard melt and snow. These features can cause the large negative differences in albedo between cities and villages, which can enhance the daytime SUHII values. This speculation can be proven by the results in cold-humid region I. In this region, the minimum daytime SUHII values occurred in the winter and autumn, and there were no significant differences between them. In addition, the differences in the albedo between cities and their corresponding villages were a unique influencing factor that was significantly correlated with the daytime SUHII values in the winter in this region ($P < 0.01$). There were obvious seasonal variations in the SUHII values in the cities in the tropical region (Figs. 2b, 2e and 3a). The SUHII values were obviously larger during the rainy season (similar to the summer and autumn) than the dry season (similar to the winter and spring). Nevertheless, there were no significant differences between the two seasons within the rainy or dry

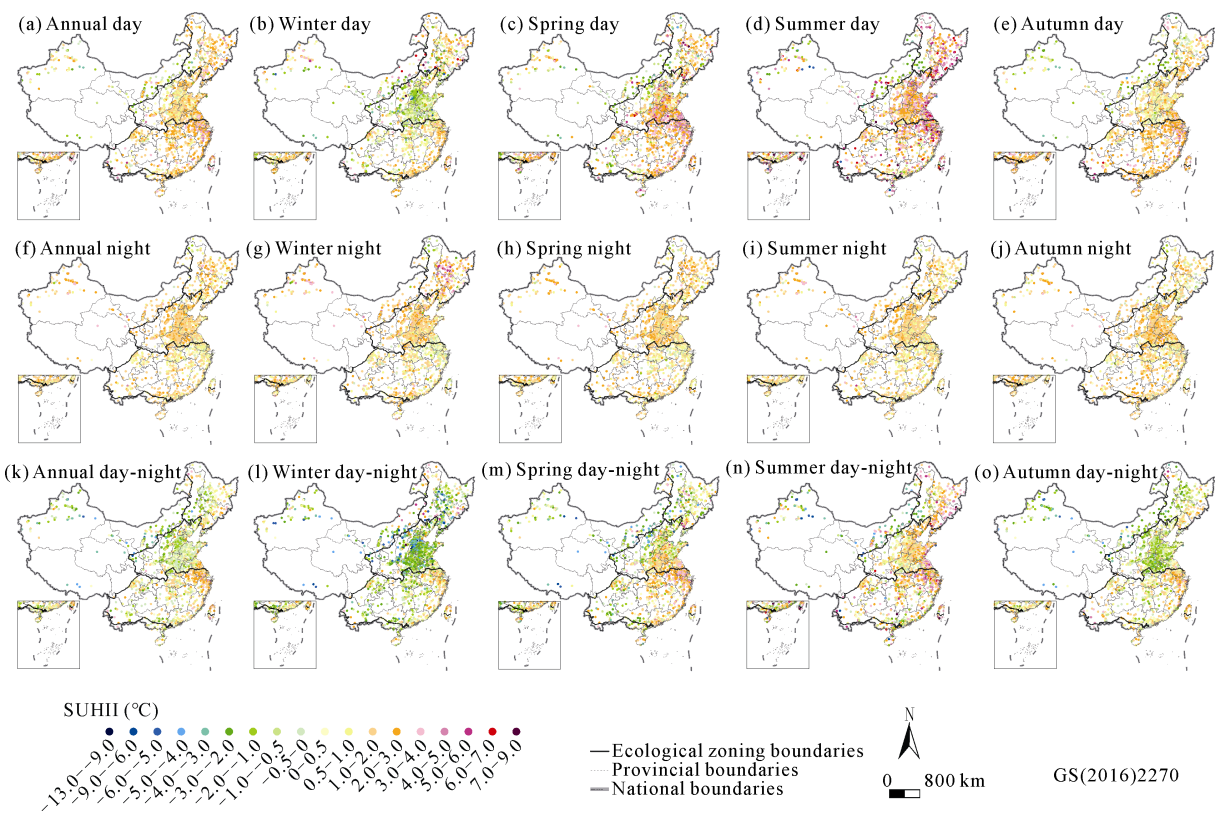

Fig. 2 Distribution of the annual and seasonal SUHIIs (surface urban heat islands intensities) during the daytime and nighttime, and the difference in the values among the five environmental regions in China in 2010. Day-night means the differences between daytime and nighttime SUHIIs.

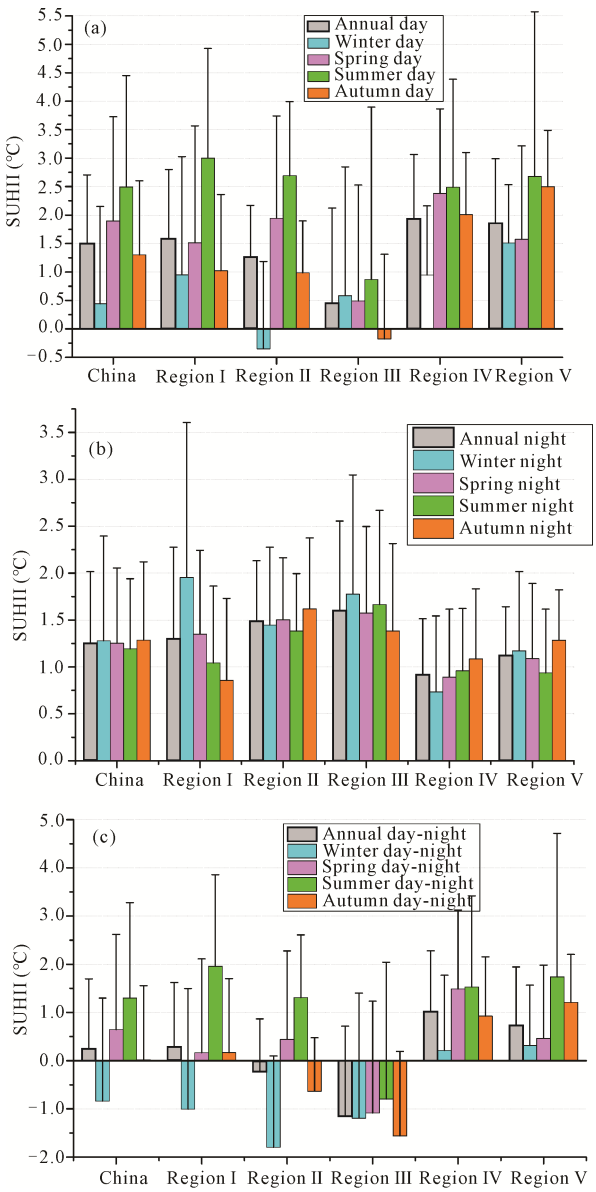

Fig. 3 Statistics of the annual and seasonal SUHIIs (surface urban heat island intensities) during the daytime and nighttime, and the differences in the values among the five environmental regions in China in 2010

periods. In Bangkok, the negative SUHII also did not change much within the dry season (Tran et al., 2006). Nevertheless, the SUHII obviously changed within the dry season for some Indian cities (Shastri1 et al., 2017). Negative SUHII values generally existed, especially during the premonsoon season in the summer and during the daytime because of the low vegetation cover in non-urban regions (Shastri1 et al., 2017).

The largest maximum SUHII values occurred in the hot-humid region V or the cold-humid region I (Figs. 4a and 5a), while the smallest maximum values occurred in the dry region III where 15.79% of the cities had negative maximum daytime SUHII values (Fig. 4a and Table 1). A daytime cold island also always existed throughout the year in other cities with typical desert climates, such as Abu Dhabi and Teheran (Lazzarini et al., 2013; Haashemi et al., 2016). The maximum daytime SUHII values mostly occurred in the summer in each region, while these values occurred least often in the winter in all regions of China except region III (Figs. 4b and 5b). Obviously, this difference can enhance the thermal stress and increase the energy consumption required for cooling in the summer.

The lowest minimum SUHII values occurred in the dry region III, while larger minimum SUHII values occurred in the hot-humid regions IV and V (Figs. 6a and 7a). The minimum SUHII values were negative and positive for most cities in the regions of North and South China, respectively. The minimum daytime SUHII values mostly occurred in the winter in each region (Figs. 6b and 7b). Obviously, these values can decrease thermal comfort and increase the energy consumption required for warming in the winter in all regions in China except for the tropical region. Both the minimum daytime SUHII and the most serious air pollution occurred in the winter. Nevertheless, SUHII can enhance air pollution, as indicated in several previous studies (Lai and Cheng, 2009; Fallmann et al., 2015).

The daytime ranges of SUHIIs were most from 0℃ to 3.5℃, generally obviously smaller in region IV than the other regions, which were most from 3.5℃ to 5.5℃ (Fig. 8a and Fig. 9).

3.1.2 Spatiotemporal changes of nighttime SUHII

A total of 96.54% of the cities had positive annual mean SUHII values in China (Table 1). Nevertheless, 50 cities had negative SUHII values, and these cities were mainly located in hot-humid or cold-humid regions (Fig. 2f). The negative values in these regions were mainly caused by the high thermal inertia from wet soil and dense vegetation. This result was consistent with previous studies at the global scale (Peng et al., 2011; Clinton and Gong, 2013). To the best of our knowledge, only one negative annual SUHII value was found in a previous study of Chinese cities (Wang et al., 2015). The vast majority studies have focused on the SUHII in only a single city, at the regional urban agglomeration scale, or have

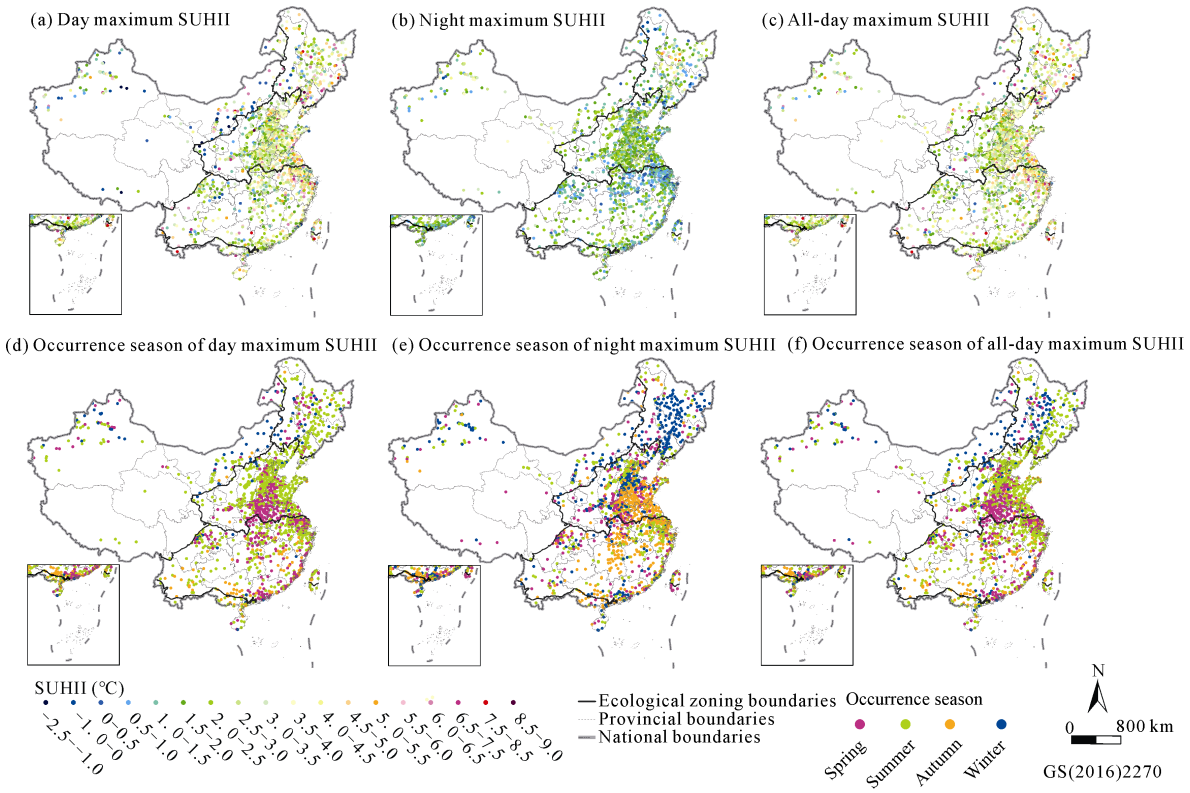

Fig. 4 Distribution of the maximum SUHIIs (surface urban heat island intensities) (a, c, e) and the occurrence seasons during the daytime, nighttime, and all-day in the five environmental regions and throughout China (b, d, f) in 2010

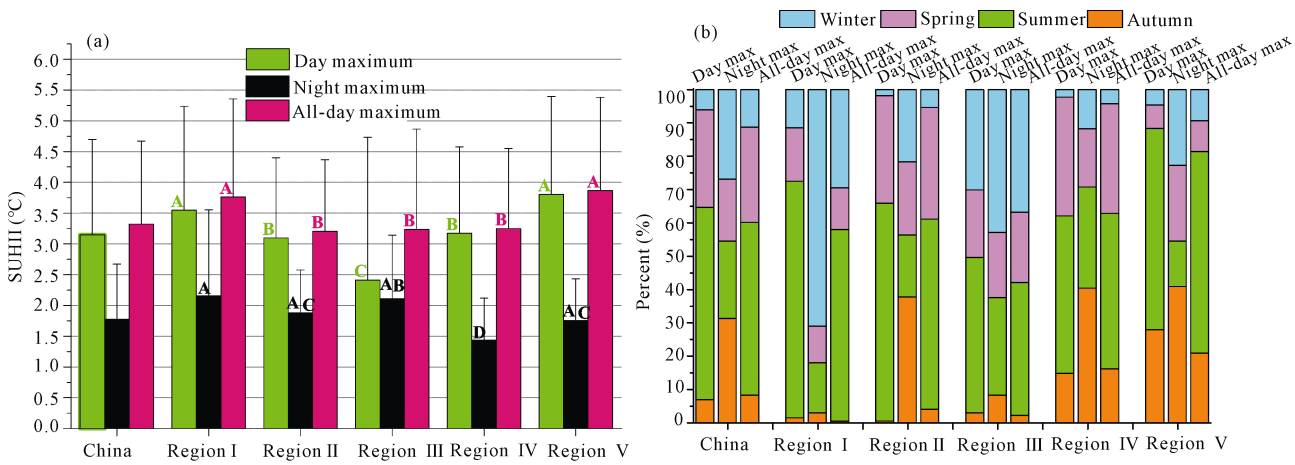

Fig. 5 Statistics of the maximum SUHIIs (surface urban heat island intensities) (a) and the seasons of occurrence during the daytime, nighttime, and all-day in the five environmental regions and throughout China (b) in 2010

considered only major cities at the national scale (Memon et al., 2009; Zhou et al., 2014). For the differences in the thermal inertia in rural environments, cities in North China had higher SUHII values than those in the south (Figs. 2f and 3b), and this result is supported a previous study (Zhou et al., 2014). The dry region III and the hot-humid region IV had the maximum and minimum SUHII values, respectively (Fig. 3b). Nevertheless, region I was identified to have the maximum mean daytime SUHII in a previous study (Zhou et al., 2014).

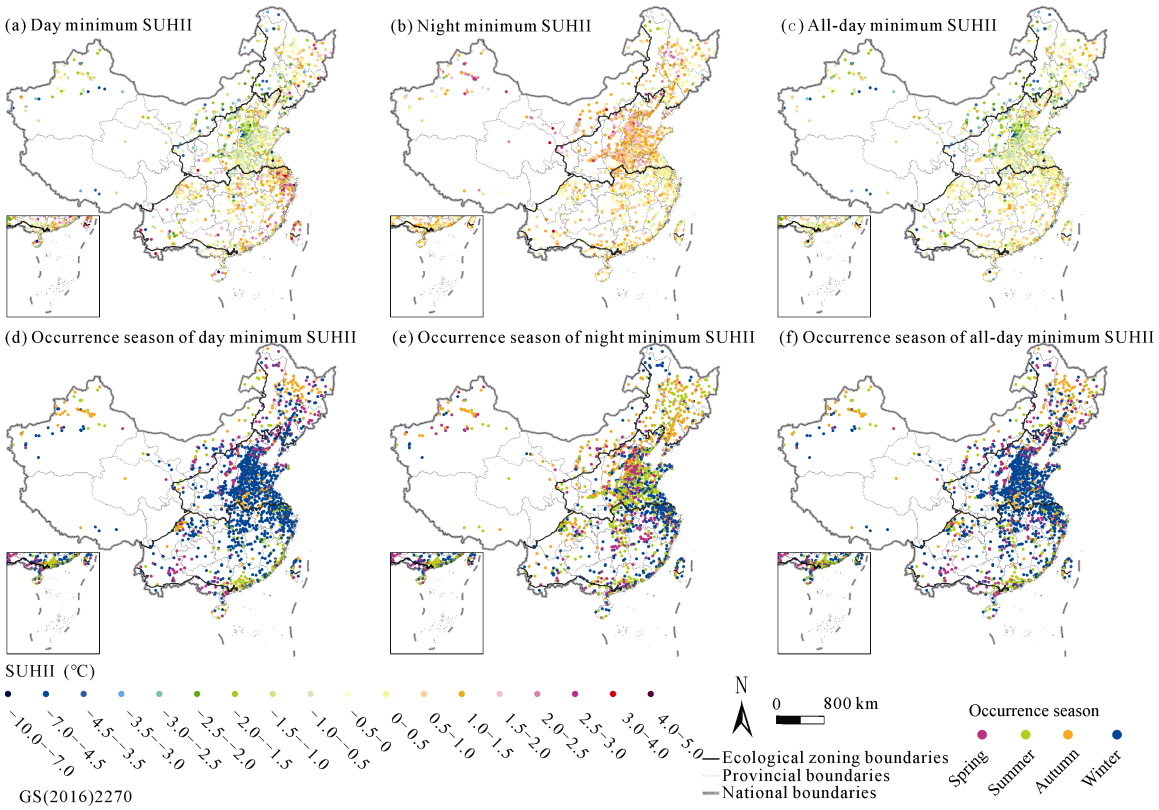

Fig. 6 Distribution of the minimum SUHIIs (surface urban heat island intensities) and the seasons of occurrence during the daytime, nighttime, and all-day in the five environmental regions in China in 2010

In general, both the seasonal and spatial variation ranges of the SUHII were lesser during the nighttime than the daytime (Figs. 2g–2j and 3b). Our finding was consistent with that of a previous study (Zhou et al., 2013), primarily because the SUHII is more influenced by human activities during the nighttime than the daytime. In addition, the seasonal variations were complex (Figs. 2g–2j and 3b), which was also found in previous results (Li et al., 2017). More negative values occurred for the seasonal SUHII means than the annual means, especially in the hot-humid region IV in the winter and spring and the cold-humid region I in the autumn (Figs. 2f–2j).

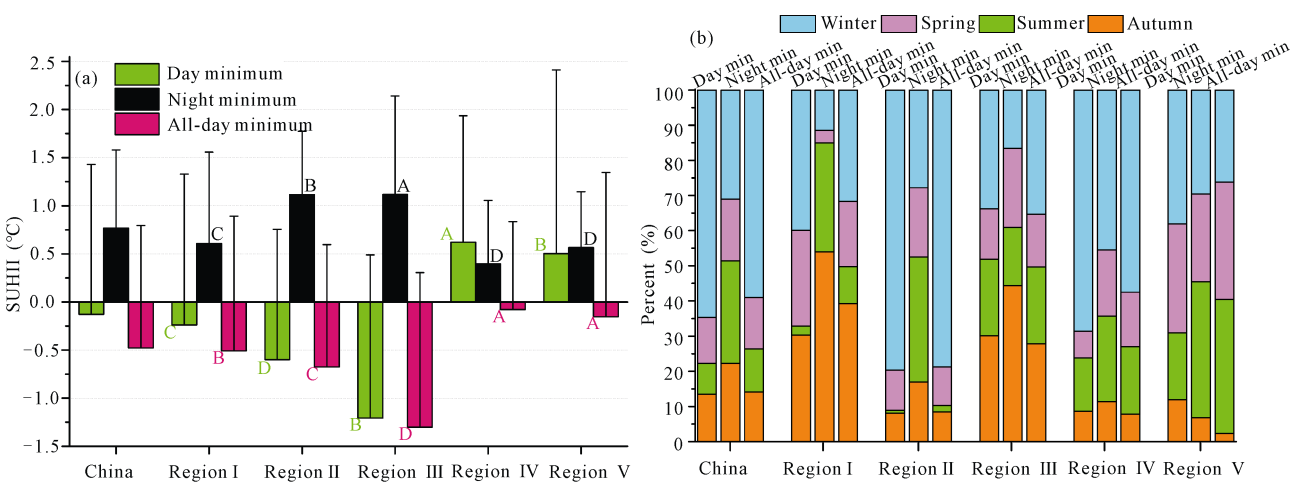

Fig. 7 Statistics of the minimum SUHIIs (surface urban heat island intensities) and the seasons of occurrence during the daytime, nighttime, and all-day in the five environmental regions and throughout China in 2010

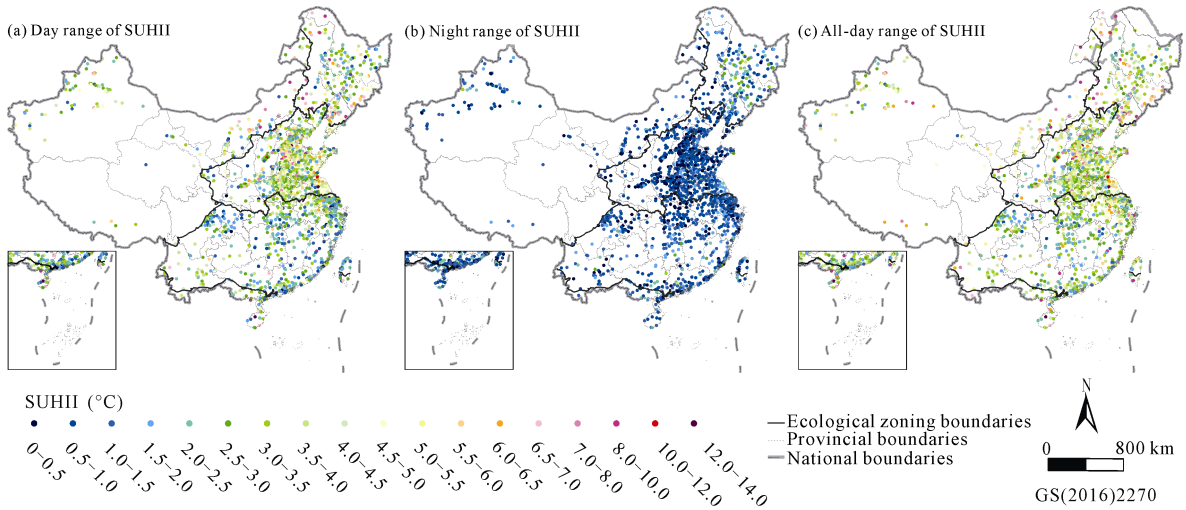

Fig. 8 Distribution of the range of SUHIIs (surface urban heat island intensities) during the daytime, nighttime, and all-day in the five environmental regions in China in 2010

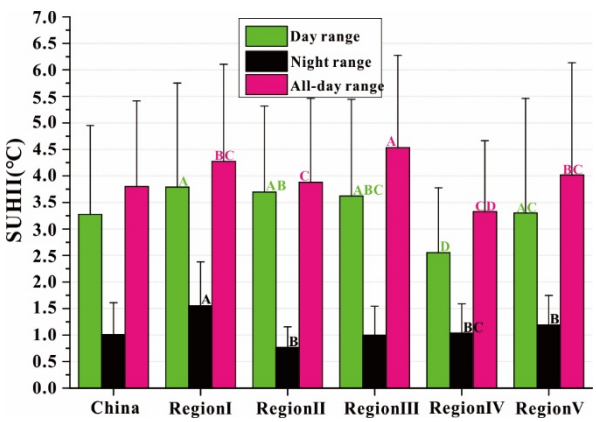

Fig. 9 Statistics of the range of SUHIIs (surface urban heat island intensities) during the daytime, nighttime, and all-day in the five environmental regions and throughout China in 2010

The spatial variation was also lesser for the maximum SUHII values during the nighttime than the daytime (Figs. 4c and 5a). Region IV had obviously lower SUHII values (Figs. 4c and 5a). Fifteen cities had negative maximum SUHII values in China, especially in the cold-humid region I where the proportion of cities with negative maximum SUHII values was 4.50% (Fig. 4c and Table 1). Similar to the complex seasonal variation, the variation in the occurrence of seasons with maximum nighttime SUHII values was still complex (Figs. 4d and 5b).

There was an obvious spatial variation in the minimum SUHII values, although the minimum values were lesser during the nighttime than the daytime (Figs. 6c and 7a). The largest minimum SUHII occurred in the dry region III, while the lowest minimum SUHII occurred in the hot-humid regions IV and V. Negative minimum nighttime SUHII values were more common, especially in the hot-humid region IV and cold-humid region I (Fig. 6c and Table 1). The rules were still complex for the seasons of occurrence of minimum nighttime SUHII (Figs. 6d and 7b).

A total of 88.18% of the cities had ranges from 0.20℃ to 1.75℃ (Fig. 8b). This range was obviously larger in region I and smaller in region II than the other regions (Figs. 8b and 9).The maximum SUHII was significantly positively correlated with the minimum SUHII during the nighttime in all regions (Table 2). Thus, it may be difficult for humans to decrease the nighttime SUHII in the summer and simultaneously increase it in the winter. Stronger relationships were found during the nighttime than the daytime. That result indicated that the mechanism was more stable for the SUHII throughout the year during the daytime than during the nighttime.

3.1.3 Spatiotemporal changes of all-day SUHII

The annual DND values in the SUHII were in the order of region IV > region V > region I > region II > region III (Fig. 3c). The annual DND of the SUHII was positive for most cities in humid and hot South China and the cold-humid region I, while it was negative in other regions, especially in the dry region III (Fig. 2k and Table 1). The negative DND of the SUHII in region I was slightly different from that found in a previous study (Zhou et al., 2016).

Table 2 Spearman correlation coefficients between the maximum and minimum surface urban heat island (SUHII) of day, night, or all-day, or between the day and night range of SUHIs for the whole China and five regions in 2010

Indices	China	Region I	Region II	Region III	Region IV	Region V
Day maximum & minimum	0.41[a]	0.27[a]	0.27[a]	0.62[a]	0.62[a]	0.43[a]
Night maximum & minimum	0.78[a]	0.83[a]	0.83[a]	0.87[a]	0.66[a]	0.65[a]
All-day maximum & minimum	0.29[a]	0.24[a]	0.22[a]	0.40[a]	0.34[a]	0.17
Day & night range	0.07[b]	0.12	0.20[a]	0.12	0.05	0.08

Notes: [a] significant at the 0.01 level; [b] significant at the 0.05 level.

Obvious seasonal variations existed in the DND of the SUHII in all regions (Figs. 2l–2o and 3c). The DND was highest in the summer in all regions and when the values were positive in all regions except region III where the DND of the SUHII was negative in all seasons (Figs. 2l–2o and 3c). At the same time, the DND was lowest in the winter for all regions, and the values were negative in North China and positive in South China (Figs. 2l–2o and 3c). The slight differences in the abovementioned content were the negative DND with small values in South China in the winter, which are similar to those measured in a previous study (Zhou et al., 2016). Due to the large number of cities examined in this study, we can find that a larger SUHII difference occurred in many cities in the Yangtze River Delta and its adjacent regions in the northern and eastern parts of region I in the summer (Fig. 3n).

The largest maximum all-day SUHII values occurred in the hot-humid region V and the cold-humid region I, while the smallest maximum values occurred in other regions (Fig. 4e and 5a). None of the maximum all-day SUHII values were negative (Table 1). The maximum all-day SUHII values mostly occurred in the summer in each region, while they occurred least often in the winter in all regions of China except in regions III and I where they occurred least often in the autumn (Fig. 4f and 5b). This difference can enhance the thermal stress and increase the energy consumption required for cooling in the summer.

Generally, the minimum all-day SUHII values could be ordered as region III < region II < region I < region V < region IV (Fig. 7a), and the same order applies for the minimum daytime SUHII values. The minimum SUHII values were negative and positive for most cities in North and South China, respectively (Fig. 6e and Table 1). The minimum all-day SUHII values mostly occurred in the winter in regions II, IV, and III, and in the autumn in regions I and III (Figs. 6f and 7b). This difference can decrease thermal comfort and increase the energy consumption required for warming in the winter in all regions of China except the tropical region.The spatial distribution pattern and statistics of the all-day SUHII differences were similar to those during the daytime (Figs. 8c and 9). The differences were not large among regions.

The maximum SUHII was significantly positively correlated with the minimum SUHII during the daytime in all regions of China except region V (Table 2). This result means that it may be difficult for humans to simultaneously decrease the maximum and increase the minimum SUHII values. The weakest relationships were found in the all-day values rather than in the daytime or nighttime values (Table 2). Moreover, a significant correlation did not exist or was weak for the daytime and nighttime ranges of SUHII in China and the five regions (Table 2). Moreover, the daytime SUHII was also insignificantly correlated with the nighttime SUHII in 50% of the cities (Table 3). That result indicated that the mechanism differed between the daytime and nighttime SUHII values. Therefore, humans should consider these values separately.

3.2 Uncertainties and limitations

Although MODIS LST data have been validated and are highly accurate in many cases and widely accepted and used, some uncertainties and issues remain, especially with respect to urban environments and rural areas with complex terrain or vegetation caused by the highly complicated spatial heterogeneity of landscape components, greater air pollution in cities and the known anisotropy issue (Clinton and Gong, 2013). To eliminate

Table 3 Spearman correlation coefficients of mean surface urban heat islands between day and night for the whole China and five regions in annual and four seasons in 2010

Period	China	Region I	Region II	Region III	Region IV	Region V
Entire year	–0.04	0.29[a]	0.09[b]	0.07	0.01	0.05
Winter	–0.17[a]	0.11	–0.26[a]	0.01	–0.14[a]	0.13
Spring	0.03	0.30[a]	0.17[a]	–0.05	0.04	0.34[b]
Summer	0.18[a]	0.30[a]	0.26[a]	0.34[a]	0.14[a]	–0.01
Autumn	0.01	0.10	0.15[a]	0.04	0.14[a]	0.19

Notes: [a] significant at the 0.01 level; [b] significant at the 0.05 level

the effect of interference factors, seasonal or annual data composited based on the daily observed values were used in this study instead of data collected at a few moments. The ready-made composite monthly mean LSTs data of China were used rather than raw daily LSTs data stored by blocks and with a large amount. The processing of monthly data mainly included mosaicking, slicing, projection transformation, mean value calculations, etc. Whether quality control information was considered was not determined, which may have introduced biases or uncertainties in our results. In the future, data collected over longer periods should be considered. Moreover, the associated determinants of SUHIIs should be explored at various scales and dimensions, especially for cities with typical spatiotemporal change laws.

4 Conclusions

We studied the intra-annual spatiotemporal variation of the SUHIIs of 1449 cities in China in 2010 based on the modified definitions of the extents of cities and their corresponding villages. Some important conclusions can be summarized as follows:

(1) During the daytime, larger annual mean SUHIIs occurred in hot-humid South China and cold-humid northeastern China, while the smallest annual mean SUHII occurred in arid and semiarid west China. The strongest SUHIIs mainly occurred in most cities in the Yangtze River Delta and coastal areas of Taiwan. The seasonal order of the SUHIIs was summer > spring > autumn > winter in all temperate regions except in the northwestern China. The SUHIIs were obviously larger during the rainy season than the dry season in the tropical region. Nevertheless, no significant differences were observed between the two seasons within the rainy or dry periods. The maximum SUHIIs mostly occurred in summer in each region, while the minimum occurred in winter.

(2) The degree of spatiotemporal variation was generally lesser for the SUHIIs during the nighttime than the daytime. The seasonal variations were complex for the nighttime SUHIIs. The mean annual SUHII was higher in North China than South China. The maximum and minimum values occurred in the northwestern region and subtropical region in South China, respectively. A certain cold island phenomenon was observed during the nighttime.

(3) The maximum SUHIIs were almost significantly positively correlated with the minimum during the daytime, nighttime and all-day in all environmental regions in China throughout the entire year and the four seasons, and this relationship was strongest and weakest during the nighttime and all-day periods, respectively.

(4) A significant correlation was not observed or was weak for the daytime and nighttime range of the SUHIIs. Moreover, the daytime SUHIIs were also insignificantly correlated with nighttime SUHIIs in 50% of the cases.

References

Chen L, Zhang M G, Zhu J et al., 2018. Modeling impacts of urbanization and urban heat island mitigation on boundary layer meteorology and air quality in Beijing under different weather conditions. *Journal of Geophysical Research–Atmospheres*, 123(8): 4323–4344. doi: 10.1002/2017 jd027501

Clinton N, Gong P, 2013. MODIS detected surface urban heat islands and sinks: Global locations and controls. *Remote Sensing of Environment*, 134: 294–304. doi: 10.1016/j.rse.2013.03.008

Fallmann J, Forkel R, Emeis S, 2015. Secondary effects of urban heat island mitigation measures on air quality. *Atmospheric Environment*, 125(Part A): 199–211. doi: 10.1016/j.atmosenv.2015.10.094 doi

Filho W L, Icaza L E, Emanche V O et al., 2017. An evidence-based review of impacts, strategies and tools to mitigate urban heat islands. *International Journal of Environmental Research & Public Health*, 14(12): 1600. doi: 10.3390/ijerph 14121600

Haashemi S, Weng Q, Darvishi A et al., 2016. Seasonal variations of the surface urban heat island in a semi-arid city. *Remote Sensing*, 8(4): 352. doi: 10.3390/rs8040352

Howard L, 1833. *Climate of London Deduced from Metrological Observations* (*3rd edition*). London: Harvey and Dorton Press.

Imhoff M L, Zhang P, Wolfe R E et al., 2010. Remote sensing of the urban heat island effect across biomes in the continental USA. *Remote Sensing of Environment*, 114(3): 504–513. doi: 10.1016/j.rse.2009.10.008

Lai L W, Cheng W L, 2009. Air quality influenced by urban heat island coupled with synoptic weather patterns. *Science of the Total Environment*, 407(8): 2724–2733. doi: 10.1016/j.scitotenv.2008.12.002

Lazzarini M, Marpu P R, Ghedira H, 2013. Temperature-land cover interactions: the inversion of urban heat island phenomenon in desert city areas. *Remote Sensing of Environment*, 130: 136–152. doi: 10.1016/j.rse.2012.11.007

Lee Y Y, Din M F M, Ponraj M et al., 2017. Overview of urban heat island (UHI) phenomenon towards human thermal comfort. *Environmental Engineering and Management Journal*, 16(9): 2097–2111. doi: 10.30638/eemj.2017.217

Li Y, Wang L, Zhang L et al., 2019. Monitoring the interannual spatiotemporal changes in the land surface thermal environment in both urban and rural regions from 2003 to 2013 in China based on remote sensing. *Advances in Meteorology*, 2019: 8347659. doi: 10.1155/2019/8347659

Li Yuanzheng, Yin Ke, Wang Yanting et al., 2017. Studies on influence factors of surface urban heat island: a review. *World Sci Tech R & D*, 39(1): 56–66. (in Chinese)

Li Yuanzheng, Yin Ke, Zhou Hongxuan et al., 2016. Progress in urban heat island monitoring by remote sensing. *Progress in Geography*, 35(9): 1062–1074. doi: 10.18306/dlkxjz.2016.09.002

Liu J, Kuang W, Zhang Z et al., 2014. Spatiotemporal characteristics, patterns, and causes of land-use changes in China since the late 1980s. *Journal of Geographical Sciences*, 24(2): 195–210. doi: 10.1007/s11442-014-1082-6

Liu J, Liu M, Tian H et al., 2005. Spatial and temporal patterns of China's cropland during 1990–2000: an analysis based on Landsat TM data. *Remote Sensing of Environment*, 98(4): 442–456. doi: 10.1016/j.rse.2005.08.012

Liu X, Hu G, Ai B et al., 2015. A normalized urban areas composite index (NUACI) based on combination of DMSP-OLS and MODIS for mapping impervious surface area. *Remote Sensing*, 7(12): 17168–17189. doi: 10.3390/rs71215863

Memon R A, Leung D Y C, Liu C H, 2009. An investigation of urban heat island intensity (UHII) as an indicator of urban heating. *Atmospheric Research*, 94(3): 491–500. doi: 10.1016/j.atmosres.2009.07.006

Mostovoy G V, King R L, Reddy K R et al., 2006. Statistical estimation of daily maximum and minimum air temperatures from MODIS LST data over the state of Mississippi. *GIScience & Remote Sensing*, 43(1): 78–110. doi: 10.2747/1548-1603.43.1.78

United Nations, Department of Economic and Social Affairs, Population Division (UN DESA PD), 2014. *World Urbanization Prospects: The 2014 Revision, Highlights*. Department of Economic and Social Affairs. Population Division, United Nations.

Peng S, Piao S, Ciais P et al., 2011. Surface urban heat island across 419 global big cities. *Environmental Science & Technology*, 46(2): 696–703. doi: 10.1021/es2030438

Ren Guoyu, Guo Jun, Xu Mingzhi et al., 2005. Climate changes of China's mainland over the past half century. *Acta Meteorologica Sinica*, 63(6): 942–956. (in Chinese)

Richards D R, Edwards P J, 2018. Using water management infrastructure to address both flood risk and the urban heat island. *International Journal of Water Resources Development*, 34(4): 490–498. doi: 10.1080/07900627.2017.1357538

Schwarz N, Lautenbach S, Seppelt R, 2011. Exploring indicators for quantifying surface urban heat islands of European cities with MODIS land surface temperatures. *Remote Sensing of Environment*, 115(12): 3175–3186. doi: 10.1016/j.rse.2011.07.003

Schwarz N, Schlink U, Franck U et al., 2012. Relationship of land surface and air temperatures and its implications for quantifying urban heat island indicators—an application for the city of Leipzig (Germany). *Ecological Indicators*, 18: 693–704. doi: 10.1016/j.ecolind.2012.01.001

Sfîcă L, Ichim P, Apostol L et al., 2017. The extent and intensity of the urban heat island in Iaşi city, Romania. *Theoretical & Applied Climatology*, 134(3–4): 777–791. doi: 10.1007/s00704-017-2305-4

Shastri1 H, Barik1 B, Ghosh S et al., 2017. Flip flop of day-night and summer–winter surface urban heat island intensity in India. *Scientific Reports*, 7: 40178. doi: 10.1038/srep40178

Shi B, Tang C S, Gao L et al., 2012. Observation and analysis of the urban heat island effect on soil in Nanjing, China. *Environmental Earth Sciences*, 67(1): 215–229. doi: 10.1007/s12665-011-1501-2

Tran H, Uchihama D, Ochi S et al., 2006. Assessment with satellite data of the urban heat island effects in Asian mega cities. *International Journal of Applied Earth Observation and Geoinformation*, 8(1): 34–48. doi: 10.1016/j.jag.2005.05.003

Voogt J A, Oke T R, 2003. Thermal remote sensing of urban climates. *Remote Sensing of Environment*, 86(3): 370–384. doi: 10.1016/S0034-4257(03)00079-8

Wang J, Huang B, Fu D et al., 2015. Spatiotemporal variation in surface urban heat island intensity and associated determinants across major Chinese cities. *Remote Sensing*, 7: 3670–3689. doi: 10.3390/rs70403670

Zhang P, Imhoff M L, Wolfe R E et al., 2010. Characterizing urban heat islands of global settlements using MODIS and nighttime lights products. *Canadian Journal of Remote Sensing*, 36(3): 185–196. doi: 10.5589/m10-039

Zhang Z, Wang X, Zhao X et al., 2014. A 2010 update of National Land Use/Cover Database of China at 1:100000 scale using medium spatial resolution satellite images. *Remote Sensing of Environment*, 149: 142–154. doi: 10.1016/j.rse.2014.04.004

Zhao L, Lee X, Smith R B et al., 2014. Strong contributions of local background climate to urban heat islands. *Nature*, 511(7508): 216–219. doi: 10.1038/nature13462

Zhou D, Xiao J, Bonafoni S et al., 2019. Satellite remote sensing of surface urban heat islands: progress, challenges, and perspectives. *Remote Sensing*, 11(1): 48. doi: 10.3390/rs11010048

Zhou D, Zhang L, Li D et al., 2016. Climate-vegetation control on the diurnal and seasonal variations of surface urban heat islands in China. *Environmental Research Letters*, 11(7): 074009. doi: 10.1088/1748-9326/11/7/074009

Zhou D, Zhao S, Liu S et al., 2014. Surface urban heat island in China's 32 major cities: Spatial patterns and drivers. *Remote Sensing of Environment*, 152: 51–61. doi: 10.1016/j.rse.2014.05.017

Zhou D, Zhao S, Zhang L et al., 2015. The footprint of urban heat island effect in China. *Scientific Reports*, 5: 11160. doi: 10.1038/srep11160

Zhou J, Chen Y, Zhang X et al., 2013. Modelling the diurnal variations of urban heat islands with multi-source satellite data. *International Journal for Remote Sensing*, 34(21): 7568–7588. doi: 10.1080/01431161.2013.821576

Zinzi M, Carnielo E, Mattoni B, 2018. On the relation between urban climate and energy performance of buildings. A three-years experience in Rome, Italy. *Applied Energy*, 221: 148–160. doi: 10.1016/j.apenergy.2018.03.192